

A Novel Approach to the Derivation of Expressions for Geometrical MTF in Sampled Systems

*R B Fagard-Jenkin, R E Jacobson and N R Axford
Imaging Technology Research Group, University of Westminster,
Harrow Campus, Watford Road. HA1 3TP. UK.*

Abstract

A novel approach to the derivation of formulae describing geometrical Modulation Transfer Function (MTF) for sampled systems is presented. The formulae are initially derived for the one dimensional case and describe performance extremes with respect to sampling pitch, aperture and spatial frequency up to the Nyquist limit. The approach is then extended to two dimensions and performance with respect to array orientation evaluated.

The formulae were tested against a high quality greyscale electronic stills camera (ECS). Predictions of the MTF were compared with measurements made using a modified edge gradient technique, sine waves and ISO 12233[1]. The results show correlation and suggest the approach is valid within the constraints given.

Introduction

A considerable contribution to the MTF of a digital device is made by the geometrical properties of the sampling array. This is defined by the dimensions of the sampling elements and the frequency at which these occur. The distance between sensitive elements is traditionally denoted the sampling pitch, p , and should not be confused with the term resolution. The width of the sensitive area of the element is denoted as the sampling aperture, s . Fill-factor may be defined as the ratio of the aperture size to the sampling pitch.

The introduction of geometrical sampling will cause a change in the MTF of a system with respect to the above parameters. Also in the two dimensional case, the use of rectangular pixels and sampling matrices, causes a variation with respect to orientation.

Mathematical Development

One Dimensional MTF

To develop a model which takes account of geometrical properties it is initially assumed that the sampling array is noiseless as is the exposing light. Consider the exposure distribution, $E(x)$ given by:

$$E(x) = a + b \cos(2\pi\omega x) \quad (1)$$

where a is mean signal level, b amplitude, ω spatial frequency per unit distance and x distance [2]. This is allowed to fall onto a sampling array which has an assumed linear response. For the purposes of derivation it is also assumed that the array and signal extends infinitely.

An idealized sampling element centred at spatial position u will collect incident light between $u \pm (s/2)$. Therefore, sampling of a single element may be modeled by straightforward integration of the signal between these points. Thus, the response, $R(u, s)$, of a single element when sampling the above signal is:

$$R(u, s) = \int_{u-\frac{s}{2}}^{u+\frac{s}{2}} E(x) \delta x \quad (2)$$

The modulation of the signal recorded by the array is dependent upon the values recorded for the maxima and minima of the input signal. This will be determined by the response of the element that is nearest the particular maximum or minimum in question and will vary according to its proximity. Establishing the possible variation in the values of recorded maxima and minima will yield the geometrical response of the array and its performance envelope.

The optimum recording of a maximum, $M_{Optimum}$, will occur when the centre of a sampling element coincides with that maximum, Figure 1. For the signal defined above it may be shown that maxima occur at $x = n/\omega$, where n is an arbitrary positive integer and therefore always at $x=0$. The optimum value that may then be recorded for a given maximum of the defined signal is:

$$M_{Optimum} = R(0, s) \quad (3)$$

The most degraded recording of a maximum will be dependent upon the pitch of the sampling array and more specifically by the proximity of the nearest element. It may be shown that for a given sampling comb, an element centre will always fall within $p/2$ of a given maximum. A straightforward conclusion is that the furthest an element

will be from a given maximum is $p/2$. Therefore, the most degraded value, $M_{Degraded}$, recorded for a given maximum will be given by:

$$M_{Degraded} = R\left(\frac{p}{2}, s\right) \quad (4)$$

Similarly, the recording of signal minima will also depend upon the pitch of the sampling array and the aperture of the elements.

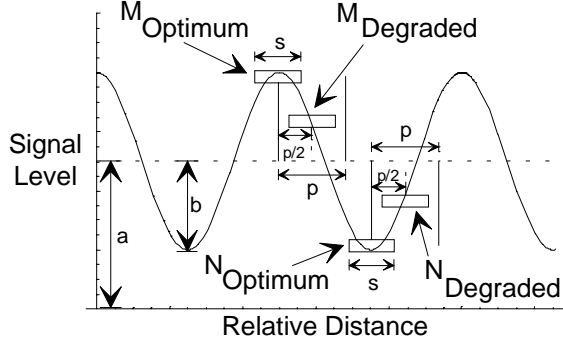


Figure 1. Parameters used in the construction of the model.

Again, optimum recording will occur when the element centre coincides with the minimum. It may be shown that minima occur at $x=(1/2\omega)+(n/\omega)$ and therefore always at $x=(1/2\omega)$. Thus, the optimum recorded value of a signal minimum, $N_{Optimum}$, will be:

$$N_{Optimum} = R\left(\frac{1}{2\omega}, s\right) \quad (5)$$

As before, the furthest an element centre may exist from a given minimum is $p/2$. The most degraded recording of a minimum, $N_{Degraded}$, may then be calculated by:

$$N_{Degraded} = R\left(\frac{p}{2} + \frac{1}{2\omega}, s\right) \quad (6)$$

Traditionally, the modulation of a sinusoidal signal, $M(\omega)$, is given by:

$$M(\omega) = \frac{Max - Min}{Max + Min} \quad (7)$$

where *Max* and *Min* denote the maxima and minima of the signal. Substituting the values above for the extremes of the maxima and minima recorded by the array, it is found that the maximum and minimum possible modulation, $M(\omega)_{Max}$ and $M(\omega)_{Min}$, will be:

$$M(\omega)_{Max} = \frac{M_{Optimum} - N_{Optimum}}{M_{Optimum} + N_{Optimum}} \quad (8)$$

$$M(\omega)_{Min} = \frac{M_{Degraded} - N_{Degraded}}{M_{Degraded} + N_{Degraded}} \quad (9)$$

where $M_{Optimum} > M_{Degraded} > N_{Degraded} > N_{Optimum}$ is assumed. Expanding and simplifying equations 8 and 9 yields:

$$M(\omega)_{Max} = \frac{b \sin(\pi\omega s)}{a\pi\omega s} \quad (10)$$

$$M(\omega)_{Min} = \frac{b \cos(\pi\omega p) \sin(\pi\omega s)}{a\pi\omega s} \quad (11)$$

The average modulation recorded by the array, $M(\omega)_{Ave}$, may be calculated as the mean of $M(\omega)_{Max}$ and $M(\omega)_{Min}$. This can be expanded to:

$$M(\omega)_{Ave} = \frac{b \cos^2\left(\frac{\pi\omega p}{2}\right) \sin(\pi\omega s)}{a\pi\omega s} \quad (12)$$

It should be noted that equations 10, 11 and 12 yield absolute recorded modulation for a given input. It is normal practice to normalize recorded modulation for a constant input with respect to the zero frequency (DC) component to produce the MTF of the system. This may be achieved by omitting variables *a* and *b* in the above equations.

The constraint relating to equations 8 and 9 limits the formulae to predicting the behaviour of undersampled arrays up to the Nyquist frequency. If *p* is defined as equal to *s*, then $M_{Optimum} = N_{Degraded}$ and $N_{Optimum} = M_{Degraded}$ at the Nyquist frequency and the constraint does not hold. Figure 2 shows the calculated maximum, minimum and average MTFs for a sampling comb with a pitch of one and sampling aperture one. This equates to a fill factor of 100%.

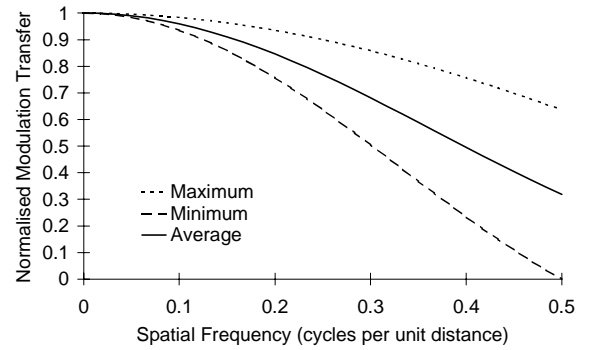


Figure 2. $M(\omega)_{Max}$, $M(\omega)_{Min}$ and $M(\omega)_{Ave}$ predicted for an array with pitch and aperture of one unit distance.

It may be seen that the derived formulae agree with Nyquist as the predicted minimum MTF falls to zero at the Nyquist frequency of the above example. The Nyquist frequency is often misquoted as the cut-off frequency of the system beyond which no response is possible. Nyquist's theorem is a limiting condition for the correct reconstruction of spatial frequencies and does not preclude a system response for frequencies above it.

The variation between the predicted maximum and minimum MTF is caused by the non-stationary nature of sampled systems. The optimum MTF is yielded when the sampling array is in phase with the target, conversely poor

performance results when the target is out of phase. This variation may be seen to increase with respect to spatial frequency. The variation may also be shown to be exacerbated by the fill factor, Figure 3. The formulae predict a larger performance envelope, the maximum MTF being increased. It may be considered an advantage as this increases the value of the average MTF, however the potential for aliasing is much higher [3].

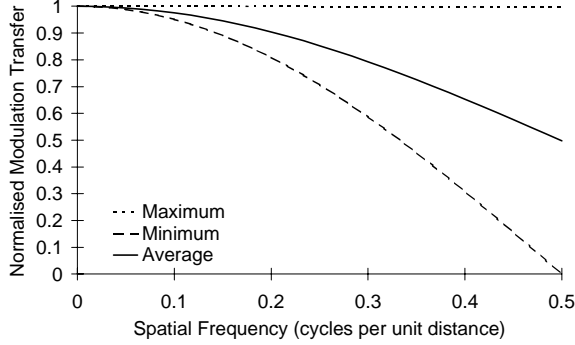


Figure 3. $M(\omega)_{Max}$, $M(\omega)_{Min}$ and $M(\omega)_{Ave}$ predicted for an array with a low fill factor ($p=1$ and $s=0.1$ unit distance).

Extension to Two Dimensions

As previously mentioned, the use of a rectangular sampling element and matrix renders a system anisotropic [4]. To take account of this, the previous model may be expanded to two dimensions and terms for the orientation of the test target added. In order to simplify derivation, the array and exposing signal is again assumed noiseless, also the sampling pitch and aperture is set to be the same in each direction.

A sinusoid, $E(x,y)$, extending infinitely in two dimensions with arbitrary rotation may be defined:

$$E(x, y) = a + b \cos(2\pi\omega x \cos(\theta) + 2\pi\omega y \sin(\theta)) \quad (13)$$

where a , b and ω take their previous definition, x and y are spatial variables and θ the orientation of the sinusoid in radians. As for the original model, a sampling element with aperture $s \times s$, centred at position (u,v) may be considered as integrating the signal over appropriate limits. The response, $R(u,v,s)$, of that element may be defined:

$$R(u, v, s) = \int_{v-\frac{s}{2}}^{v+\frac{s}{2}} \int_{u-\frac{s}{2}}^{u+\frac{s}{2}} E(x, y) \delta x \delta y \quad (14)$$

Using the same approach, variation in modulation recorded by the array is examined by considering the fate of signal maxima and minima. As the sampling array extends infinitely this is possible by observing a single row of elements which is centered on the generated exposure at $y=0$.

As previously stated, optimum recording of a maximum will occur when the centre of a sampling element

coincides with that maximum. It may be shown that, when $y=0$, $E(x,y)$ has maxima at:

$$x = \frac{n}{\omega \cos(\theta)} \quad (15)$$

Thus, a signal maximum will occur at $E(0,0)$ and the optimum recording, $M_{Optimum}$, may be defined:

$$M_{Optimum} = R(0,0,s) \quad (16)$$

Again it may be shown that a sampling element will fall within $p/2$ of the maximum. The most degraded recording of a maximum, $M_{Degraded}$, will then be given by:

$$M_{Degraded} = R\left(\frac{p}{2}, 0, s\right) \quad (17)$$

The recording of minima occurs in a similar manner. When $y=0$ it may be shown that minima of $E(x,y)$ occur at:

$$x = \frac{1}{2\omega \cos(\theta)} + \frac{n}{\omega \cos(\theta)} \quad (18)$$

and that the first minimum occurs at $x=1/(2\omega \cos(\theta))$. The optimum recording of a minimum, $N_{Optimum}$, may be defined:

$$N_{Optimum} = R\left(\frac{1}{2\omega \cos(\theta)}, 0, s\right) \quad (19)$$

It may be shown that a sampling element will occur within $p/2$ of the minimum and thus the most degraded recording of the minimum, $N_{Degraded}$, is defined by:

$$N_{Degraded} = R\left(\frac{p}{2} + \frac{1}{2\omega \cos(\theta)}, 0, s\right) \quad (20)$$

As for the one dimensional model, the maximum and minimum MTFs may be shown to be given by equations 8 and 9 with similar constraints. Substituting the new values of recorded maxima and minima into the equations it is found:

$$M(\omega)_{Max} = \frac{b \cdot c(\omega)}{a\pi^2 \omega^2 s^2} \quad (21)$$

$$M(\omega)_{Min} = \frac{b \cos(\pi\omega p \cos(\theta)) \cdot c(\omega)}{a\pi^2 \omega^2 s^2} \quad (22)$$

where $c(\omega)=2 \csc(2\theta) \sin(\pi\omega s \cos(\theta)) \sin(\pi\omega s \sin(\theta))$ and $0 < \theta \leq \pi/4$. For reasons as given previously for the one dimensional model, the use of these formulae is restricted to undersampled systems up to the Nyquist frequency. Again, normalized MTFs may be produced by omitting a and b .

The fundamental influence of the orientation of the test target may be shown by examining the change in MTF. Figure 4 shows that as the target is rotated both the maximum and minimum MTF increases, though by a much

decreased amount in the case of the maximum MTF. The precise progression of the performance as the target is rotated may be examined by plotting modulation versus target angle for a single spatial frequency, Figure 5.

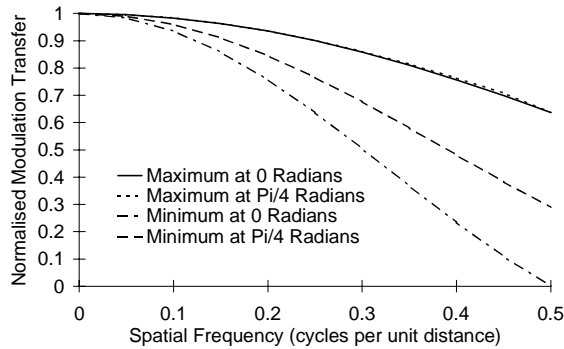


Figure 4. $M(\omega)_{Max}$ and $M(\omega)_{Min}$ predicted for a sampling array with pitch and aperture of one unit distance in each direction, at 0 and $\pi/4$ radians.

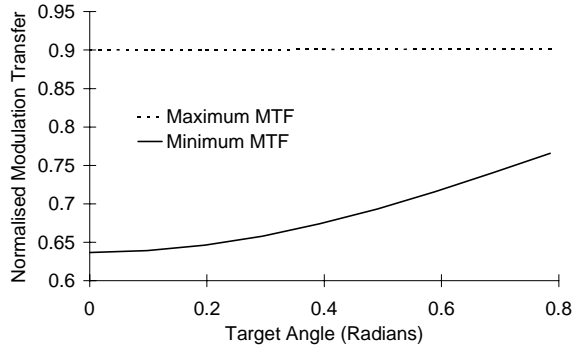


Figure 5. $M(\omega)_{Max}$ and $M(\omega)_{Min}$ plotted with respect to target orientation for a sampling array with pitch and aperture of one unit distance in each direction for a spatial frequency of 0.25 cycles per unit distance.

The model predicts that interaction between the spatial frequency imaged and the orientation exists, Figure 6. As spatial frequency increases, the orientation has a greater effect. This is illustrated by the increased variation in the curves for higher spatial frequencies. For the DC component, orientation is shown to have no influence indicated by the constant value for the curve. This agrees with intuition, as no variation in imaged density would be expected if a uniform grey patch were rotated.

The interaction of spatial frequency and orientation is important as it suggests a further cause of measurement noise at high spatial frequencies. Slight mis-orientation of test targets will cause increased deviation of the measured MTF from the true value at high spatial frequencies. Furthermore, this deviation will be positive and compound the bias introduced by random noise [5].

Fill factor is predicted to have little interaction with the orientation of the test signal. Figure 7 shows the minimum MTF for sampling arrays with fill factors of 100% and 1% at orientations of 0 and $\pi/4$ radians. Whilst initially it may

appear that for a low fill factor there is a greater increase in MTF as the sinusoid is rotated, this is eliminated if the original response of the sampling array at zero radians is considered. This may be achieved by plotting the increase in MTF for given angle as a ratio of the MTF with no rotation, Figure 8.

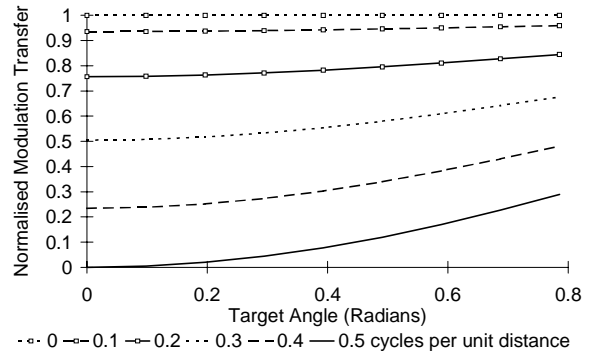


Figure 6. $M(\omega)_{Min}$ plotted against θ for various spatial frequencies. The sampling array has pitch and aperture of one unit distance in each direction.

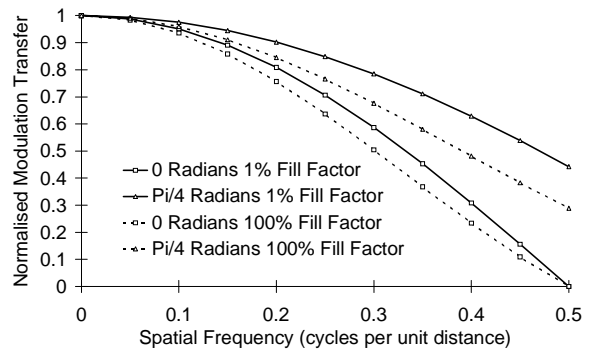


Figure 7. Minimum predicted MTF for arrays with fill factors of 100% and 1% at orientations of 0 and $\pi/4$ radians.

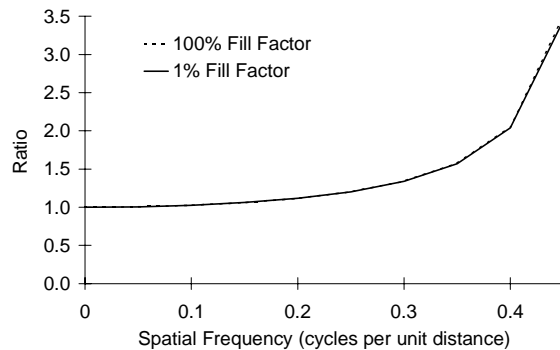


Figure 8. Increase in MTF plotted as a ratio of the MTF at 0 radians for arrays with fill factors of 100% and 1%.

As may be seen the ratio of the increase in the MTF with respect to that when it is not rotated is virtually identical, indicating that there is no or little interaction between fill factor and orientation.

Experimental Confirmation and Discussion

To confirm the above approach to the calculation of geometrical MTF, a modified edge technique, the ISO 12233 standard and a sine wave method were used to determine the minimum, maximum and average MTFs of the Kodak DCS 420m (monochrome) in combination with a Nikon AF 28mm f2.8 D lens.

Test targets were mounted on a 3m optical bench with an arrangement of micro-positioners to adjust translation and rotation in the plane of the target. The stated accuracy of the micrometers was $\pm 2\mu\text{m}$ in linear translation and ± 5 minutes of arc in rotation. Two Photoflood 200W tungsten lamps provided even illumination. The DCS 420 was rigidly mounted on the bench so that the optical axis of the camera was orthogonal to the plane of the target. The distance between the test target and camera was used to calculate the magnification of the arrangement as 1.7×10^2 .

After positioning and rotating the target as required, the camera's autofocus system was used to focus. Automated focusing was preferred over manual due to its increased consistency. The lens was set at an aperture of f5.6 and used in combination with the Tiffen infra-red absorbing filter provided with the camera. The speed setting of the camera was adjusted to ISO 200 and the correct exposure determined using the camera meter in spot mode with a Kodak R-27 greycard placed in the plane of the target.

After making exposures as desired, images were downloaded to an IBM compatible PC, via the Adobe Photoshop plug-in provided, as 8 bit data. Relevant data was extracted and then converted into effective exposure units [6] using the transfer function of the device determined with a Kodak Q-13 greyscale under similar circumstances.

The MTF of the system was calculated using each image according to the details given later. The lens MTF was investigated using an Ealing Optics EROS 200. This component was removed from the system MTF in the usual manner to yield that of the charged coupled device (CCD).

The manual accompanying the DCS420 specifies the sampling pitch of the CCD to be $9\mu\text{m}$. The fill factor and thus the aperture of the elements is not specified, although a typical value is 90%. Assuming square elements this value was used to determine the aperture size as $8.53\mu\text{m}$.

One Dimensional MTF

To determine maximum and minimum MTFs an edge target was produced using a Hewlett Packard 6MP laser printer. To avoid effects caused by half-toning the edge was arranged in the direction of printing and designed to have a transition from the maximum possible density to page white. A number of measurements were made along the length of the edge to ensure a consistent density. The use of a laser printed edge, whilst not ideal, is possible because of the low magnification of the system which ensures the frequency response of the target is constant over the desired range. This may be confirmed easily using reflection microdensitometry.

The target was positioned in the centre of the field of view of the camera. Exposures were made and examined in

order to align the orientation of the target with the array. Images were made, using the procedure described above, translating the target in $50\mu\text{m}$ intervals with the micro-positioners. This corresponded to the image of the edge advancing $0.85\mu\text{m}$ across the CCD. The images were then downloaded and corrected as above. A mean edge profile was extracted from each by averaging columns in order to reduce noise. MTFs were calculated in the usual manner [7] and the maximum and minimum response selected. In addition all responses were averaged to produce a mean.

To calculate the SFR of the device, the above target was rotated approximately 5° and an exposure made. This image and the previously calculated transfer function were used as the input image and *Opto-Electronic Conversion Function* for the ISO 12233 plug-in. All results were corrected for the component of lens MTF and compared to those predicted.

Figure 9, shows a reasonable degree of correlation between the predicted and determined values. The mean measured MTF however corresponds better to $M(\omega)_{Ave}$ than does the SFR. Further work is needed to explain this result.

Correlation of the results might be improved as it is possible that the translation of the edge image was not of sufficient subtlety to invoke the maximum and minimum response of the array.

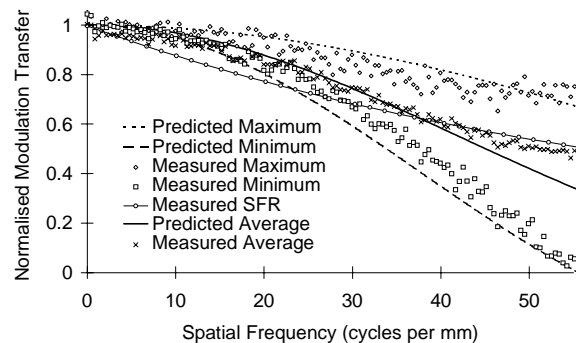


Figure 9. Comparison of the predicted performance envelope with that determined for the Kodak DCS420m.

In this work no account has been taken for the effect of an optical pre-filter or system electronics. As these effects increase for a given system, the MTF will depart from the geometrical component. Further inaccuracies may be contained in the predicted MTFs due to the use of an estimated value of aperture and measurement of the lens MTF.

Two Dimensional MTF

Confirmation of the two dimensional case is challenging for a number of reasons. To validate the results it is necessary to measure slight changes in the recorded modulation of single frequencies close to the Nyquist limit of the system with respect to orientation. This is because the formulae predict the largest variation in values at this point and present the best opportunity to evaluate this phenomenon. It is therefore important that the noise threshold and the implementation of the measurement methodology in two dimensions be carefully considered.

Methods which involve the simulation of white noise yield two dimensional responses with relative ease [8]. It is not possible, however, to determine performance extremes as the effects of the non-stationary nature of the array are usually integrated over the area of the target. Furthermore, they generally suffer from noise [8]. Edge gradient techniques are difficult to implement at arbitrary angles due to the discrete nature of the sampling array. Though labour intensive, the use of a sinusoidal test pattern is advantageous. The effect of orientation may easily be examined for a single spatial frequency with low measurement noise. Also, the performance envelope of the system may be evaluated as the effects of aliasing and alignment of the target and array can be distinguished.

Exposures of a Sine Patterns [9] M13-60 sinusoidal target were made as before at 10° intervals between 0° and 40° and also at 45°. After downloading and correction, maxima and minima were extracted from a single sinusoidal patch (0.75 cycles per mm on target) for each image. The variation in the maxima and minima was found and used to calculate maximum and minimum recorded modulation. These values were then corrected for the effects of the lens and input modulation of the sinusoid in the usual manner and compared to those predicted by the formulae, Figure 10.

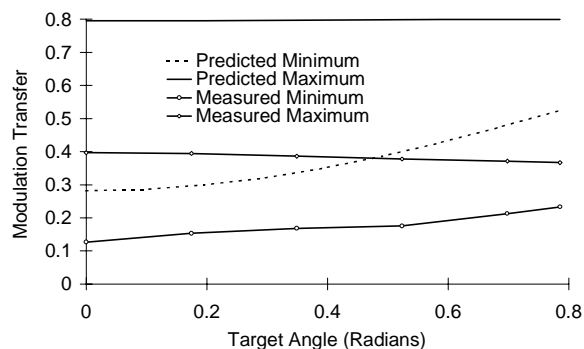


Figure 10. Recorded modulation with respect to orientation

Initially the results appear to have a poor correlation. The necessity, however, of measuring the effects close to the Nyquist frequency produces a high chance of systematic errors. Error in the MTF of the lens and inaccurate focusing could combine to produce a consistent deviation. Considering this, it is possible to normalize the curves with respect to the response of the system when the target is not rotated in order to remove any deviation, Figure 11.

After normalization, the results have better correlation. Both the minimum and maximum MTFs follow the trend suggested by the formulae. Though containing measurement error these results confirm that the minimum MTF is affected more than the maximum and that the MTF increases as the target is rotated. Measurement error is not only caused by random fluctuations but also the finite size of the test target. To produce all possible recorded extremes of maxima and minima requires a large number of input cycles and thus a large test target area.

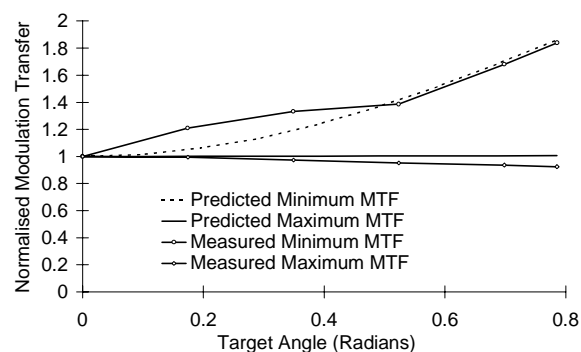


Figure 11. Normalised results with respect to orientation.

These results do not fully validate the formulae. Many other aspects require testing, such as interaction between spatial frequency and orientation. Further work is necessary to refine measurement techniques and confirm results.

Conclusion

Formulae to predict the geometrical MTF of sampled systems have been presented and an attempt made to experimentally validate them. The one dimensional results shown good correlation. Some trends predicted by the two dimensional formulae have been confirmed but further work is necessary to improve measurement techniques in order to fully validate results.

Acknowledgments and Thanks

This work was funded by the Engineering and Physical Science Research Council (EPSRC) in collaboration with Kodak Ltd., Grant Number 96592576. The primary author thanks J Frankland for support during the production of this work.

References

1. D Williams, Benchmarking of the ISO 12233 Slanted-edge Spatial Frequency Response (SFR) Plug-in, *Proc. 51st IS&T PICS Conf.*, 133-136, (1998).
2. J C Dainty and R Shaw, *Image Science*, Academic Press, London, UK. (1974).
3. M Kriss, Tradeoff Between Aliasing Artifacts and Sharpness in Assessing Image Quality, *Proc. 51st IS&T PICS Conf.*, 247-256, (1998).
4. D Lake, Evaluating Cameras: About MTF, *Advanced Imaging*, 16-18, (May 1996).
5. E S Blackman, *Photogr. Sci. Eng.*, **9**, 314-318, (1965).
6. C N Nelson, F C Eisen and G C Higgins, Effect of Non-Linearities when Applying Modulation Transfer Techniques to Photographic Systems, *Proc. SPIE*, **13**, 127-134, (1968).
7. R A Jones, *Photogr. Sci. Eng.*, **11**, 102-106, (1967).
8. M Gouch and M Roe, Image MTF Analysis Using Grain Noise, *Proc. SPIE*, **1987**, 96-102, (1993).
9. R Lamberts, Sine Patterns, 236 Henderson Drive, Penfield, New York 14526, USA.